University of Hertfordshire UH 25 Research Archive

Citation for published version:
Charlotte A. Hall, Helen L. Lydon, Christopher H. Dalton, J. Kevin Chipman, John S. Graham, and Robert P. Chilcott, 'The percutaneous toxicokinetics of Sulphur mustard in a damaged skin porcine model and the evaluation of WoundStat™ as a topical decontaminant', *Journal of Applied Toxicology,* Vol. 37 (9): 1036-1045, July 2017.

DOI:
https://doi.org/10.1002/jat.3453

Document Version:
This is the Accepted Manuscript version.
The version in the University of Hertfordshire Research Archive may differ from the final published version.

Copyright and Reuse:
© 2017 John Wiley & Sons Ltd.
This article may be used for non-commercial purposes in accordance with Wiley Terms and Conditions for Self-Archiving.

Enquiries
If you believe this document infringes copyright, please contact the Research & Scholarly Communications Team at rsc@herts.ac.uk

The percutaneous toxicokinetics of sulphur mustard in a damaged skin porcine model and the evaluation of WoundStat™ as a topical decontaminant

Short title: Evaluation of WoundStat™ as a topical decontaminant

Authors
Charlotte A. Hall[a,b,*], Helen L. Lydon[a,b,†], Christopher H. Dalton[c], J. Kevin Chipman[b], John S. Graham[e] and Robert P. Chilcott[a,d]
Affiliations
[a]*CBRN & Chemical Toxicological Research Group, Centre for Radiation, Chemical and Environmental Hazards, Health Protection Agency, Chilton, UK*
[b]*School of BioSciences, University of Birmingham, Birmingham, UK*
[c]*Biomedical Sciences, Dstl Porton Down, Salisbury*
[d]*Research Centre for Topical Drug Delivery and Toxicology, University of Hertfordshire, Hatfield, UK*
[e]*Medical Toxicology Branch Analytical Toxicology Division, U.S. Army Medical Research Institute of Chemical Defense, Aberdeen Proving Ground, MD 21010, USA*

*Current address for author; Research Centre in Topical Drug Development and Toxicology, University of Hertfordshire, Hatfield, UK, AL10 9AB

†Current address for author; Division of Trauma and Orthopaedic Surgery, University of Cambridge, Addenbrooke's Hospital, Cambridge, CB2 2QQ

Address correspondence to Robert P. Chilcott, Department of Pharmacy, University of Hertfordshire, Hatfield, UK, AL10 9AB
r.chilcott@herts.ac.uk

Keywords

vesicants, pig, topical decontaminants, haemostats, laser Doppler imaging, skin reflectance spectroscopy

Abstract

This study used a damaged skin, porcine model to evaluate the *in vivo* efficacy of WoundStat™ for decontamination of superficial (non-haemorrhaging), sulphur mustard-contaminated wounds. The dorsal skin of 12 female pigs was subjected to controlled physical damage and exposed to 10 µL ^{14}C-radiolabelled sulphur mustard (^{14}C-SM). Animals were randomly assigned to either a control or a treatment group. In the latter, WoundStat™ was applied 30 s post exposure and left *in situ* for 1 h. Skin lesion progression and decontaminant efficacy were quantified over 6 hours using a range of biophysical measurements. Skin, blood and organ samples were taken *post mortem* for histopathological assessment, ^{14}C-SM distribution and toxicokinetic analyses. Application of SM to damaged skin without decontamination was rapidly followed by advanced signs of toxicity, including ulceration and decreased blood flow at the exposure site in all animals. WoundStat™ prevented ulceration and improved blood flow at the exposure site in 100% of decontaminated animals (*n*=6). Furthermore, significantly smaller quantities of ^{14}C-SM were detected in the blood (45% reduction), and recovered from skin (70% reduction) and skin surface swabs (99% reduction) at 6 hours post-challenge. Overall, the distribution of ^{14}C-SM in the internal organs was similar for both groups, with the greatest concentration in the kidneys, followed by the liver and small intestine. WoundStat™ significantly reduced the amount of ^{14}C-SM recovered from the liver, a key organ for SM metabolism and detoxification. This study demonstrates that WoundStat™ is a suitable product for reducing the ingress and toxicity of a chemical warfare agent.

Short abstract

Application of ^{14}C-radiolabelled sulphur mustard (^{14}C-SM) to damaged pig skin without decontamination resulted in advanced signs of toxicity with rapid onset (*n*=6). Application of WoundStat™ post exposure prevented or delayed signs of toxicity in all decontaminated animals (*n*=6) and improved perfusion at the exposure site, while significantly smaller quantities of ^{14}C-SM were detected in the blood and recovered from the skin. This study demonstrates that WoundStat™ is suitable for reducing the ingress and toxicity of a vesicant agent.

Introduction

Sulphur mustard (SM) is an incapacitating chemical warfare (CW) agent that poses a threat to both civilian and military populations (Wattana and Bey 2009). Despite extensive research since its first reported use almost 100 years ago in Ypres, Belgium (Ireland, 1926) the exact mechanism of SM toxicity remains elusive and therapy is limited to symptomatic treatment (Jenner and Graham, 2013; Rice, 2016, 2003). Dermal injuries following SM exposure are dose-dependent and characterised by erythema, blister formation and ulcerations that are slow to heal (Vogt *et al*., 1984; Petrali and Oglesby-Megee, 1997; Kehe and Szinicz, 2005). Additionally, there is a dose-dependent, latent period between SM exposure and the signs of toxicity for intact (undamaged) skin (Graham *et al*., 2005), which is attributed to cellular processes, including DNA damage or inflammatory-mediated responses (Arroyo *et al*., 2000; Papirmeister *et al*., 1985). However, there is little information regarding dermal sequelae following SM exposure of compromised skin.

In vitro studies have shown that both the rate and the total amount of SM penetration are significantly enhanced through damaged skin (Lydon *et al*., 2017), Thus, it is conceivable that the progression of SM injury could be more rapid if the skin were damaged. Whilst a number of *in vivo* studies have evaluated decontamination of SM-exposed undamaged skin (Chilcott *et al*., 2007; Taysse *et al*., 2011, 2007; Wormser *et al*., 2002), data on the decontamination of SM-exposed damaged skin are limited to visual scoring of gross lesions and changes in leukocyte number (Gold *et al*., 1994). This paucity of data poses a substantial problem in the establishment of best practice protocols for decontaminating individuals who have abraded skin or have sustained blast or similar injuries. Furthermore, current decontamination regimes are contraindicated for intra-wound use and may adversely affect wound healing (Gibbs and Pooley, 1994; Walters *et al*., 2007). Therefore, a product suitable for halting bleeding and decontaminating wounds or abraded skin would be of significant clinical benefit. Previous studies have demonstrated that WoundStat™, a granular haemostat, has comparable efficacy to in-service military decontaminants (fuller's earth and M291) in the decontamination of both undamaged and damaged skin (Dalton *et al*., 2015, Lydon *et al*., 2017). Additionally, WoundStat™ maintains its haemostatic capability in the presence of toxic chemicals, including SM, *in vitro* (Hall *et al*., 2015).

The domestic pig is an established model for evaluating SM-induced cutaneous lesions in normal skin (Monteiro-Riviere and Inman, 1997; Chilcott *et al*., 2007; Graham *et al*., 2000; Price *et al*., 2009; Smith *et al*., 1997), producing epidermal microblisters that are comparable with the blistering seen in humans (Brown and Rice, 1997; Mitcheltree *et al*., 1989). However, the effects of removing the skin barrier layer (*stratum corneum* [SC] and epidermis) on SM lesion progression are not well characterised. Therefore, this study characterised early progression of SM dermal injuries when applied to damaged porcine skin and evaluated the decontaminant efficacy of WoundStat™.

Materials and Methods

Chemicals

The storage and use of CW agents was in full compliance with the Chemical Weapons Convention (1993). Sulphur mustard and its radiolabelled (^{14}C) analogue were custom synthesised by TNO Defense (Rijswijk, Netherlands). The purity of the agents was determined to be 99.2% and >97% for SM (nuclear magnetic resonance analysis) and ^{14}C-SM (gas chromatography–mass spectrometry and high-performance liquid chromatography analysis), respectively. The ^{14}C-SM solution was diluted with unlabelled SM to yield a working solution with a nominal activity of 11 mCi g^{-1}, which was stored for up to 3 months at 4°C.

Animal model

The use of animals was in accordance with the Animals (Scientific Procedures) Act (1986). Twelve pigs (*Sus scrofa*, large white strain, females) were purchased from a reputable supplier (weight range 15–25 kg, mean weight 19.5 kg) and were kept in pairs with access to food and water *ad libitum*. Animals were housed in a temperature (22–24°C) and humidity (45–65%) controlled environment under a 12 h/12 h light/dark cycle.

Animals were sedated (6 mL, Hypnoval®, Roche Products Ltd.) prior to induction of anaesthesia using 3.5–5% isoflurane. Following endotracheal tube placement, anaesthesia (1.5–2.5% isofluorane) was maintained and the carotid artery and the internal jugular vein were surgically cannulated to provide access for arterial blood sampling and intravenous administration of anaesthetic. Alfaxan (alfaxalone; 10 mg mL^{-1} Vétoquinol UK Ltd.) was administered at a rate of 1.0–1.2 mg kg^{-1} h^{-1} for the remainder of the study. Adjustments were made to the anaesthetic dose throughout the study to ensure that an appropriate level of consciousness was maintained. Physiological parameters (pulse oximetry, capnography, core body temperature, electrocardiogram, respiratory rate and blood pressure) were monitored throughout the study using a Propaq® Encore 204-EL device (Welch Allyn [UK] Ltd.).

Experimental procedures

Animals were randomly assigned to either the SM control (SM-exposed no decontamination) or decontamination (SM-exposed with WoundStat™ decontamination) group at the start of the study (n=6 for each group). The dorsum of all animals was close clipped and up to four dosing rings were attached to identify treatment sites. Treatment sites were randomly assigned among multiple dorsal sites, using a Latin square design, to reduce the influence of anatomical bias. In the SM control group, the treatment sites evaluated the effect of skin damage alone (damaged site) and skin damage in combination with SM exposure (SM site). A treatment site that was neither damaged nor SM-exposed (control site) was included as a negative control. Treatment sites for the decontamination group evaluated the effect of (i) skin damage alone (damaged site), (ii) skin damage in combination with WoundStat™ (WS site), and (iii) skin damage in combination with WoundStat™ and SM exposure (WS + SM site). As in the SM control group, a treatment site that was neither damaged nor SM-exposed (control site) was included as a negative control.

For damaged skin treatment sites, a small (~3 cm^2) section of skin was removed using a dermatome (Humeca Model D42, Eurosurgical Ltd.) to a nominal

depth of 100 μm. Any resulting transient, punctuate bleeding was swabbed with cotton gauze soaked in saline to remove extraneous material, such as dried blood.

Baseline biophysical measurements and blood samples were taken following a 30 min stabilisation period post surgery and immediately prior to SM exposure. A multi-vesicating (10 μL) dose of ^{14}C-SM was applied as a discrete droplet to one damaged skin site. In the WoundStat™ decontamination group, 2 g of WoundStat™ was applied to the SM-exposure site 30 s later. WoundStat™ was also applied to an unexposed damaged skin site to determine whether WoundStat™ would cause adverse reactions *in vivo.* Both SM and WoundStat™ were removed from the treatment sites using cotton swabs and surgical gauze after 60 min so that biophysical measurements could be made. To aid the recovery of WoundStat™, 1 mL of sterile water was applied to the haemostat immediately before removal, so that it formed a clay-like mass. The cotton swabs, surgical gauze and WoundStat™ were retained for radiometric analysis.

Biophysical measurements

Biophysical measurements were made pre-exposure (baseline) and at hourly intervals from 60 min post-exposure (approximately 1 min after the removal of WoundStat™ and/or SM from treatment site) until the study end (6 h post exposure). Dermal blood flow was measured using a laser Doppler line scanner (LDLS, Moor Instruments) as previously described (Brown *et al*., 1998). Repeat line scanner images were taken in triplicate (200 ms per line). The region of interest (ROI), defined as the area within the dosing ring, was exported for further analyses. Skin colour changes were assessed using skin reflectance spectroscopy (SRS; CM-2600d, Konica Minolta). Standard CIELAB colour space values (L*a*b*) were obtained as previously described (Chilcott *et al*., 2000). Skin surface temperature was measured using infrared thermography (FLIR SC620; FLIR Systems). Thermographs of the treatment sites were obtained in triplicate. The ROI was selected and exported (ThermaCAM™ Researcher software; FLIR Systems Ltd.) for further analyses. Skin barrier integrity was evaluated as a function of transepidermal water loss (TEWL; AquaFlux AF200; Biox Systems) as previously described (Chilcott *et al*., 2000). Where appropriate, all equipment was calibrated before use in accordance with the manufacturer's guidelines.

Blood and tissue sampling

Arterial blood samples (2 mL) were acquired for toxicokinetic analysis prior to SM exposure, immediately after SM dosing, and at hourly intervals thereafter. Samples were stored in 3.2% sodium citrate vials (Teklab Ltd.) at -20°C prior to analysis. Animals were euthanised with a lethal dose of Dolethal (Vétoquinol UK Ltd.) at 6 h post-exposure. The skin from each treatment site was excised and representative samples were taken for histological and radiometric analysis. *Post mortem* examinations were performed, during which the main organs (brain, heart, lung, liver, kidney, pancreas and spleen) were removed and weighed, and representative samples were taken for radiometric analysis. Representative sections of small intestine were also taken for radiometric analysis.

Quantification of 14C radiolabel

Skin samples from treatment sites were solubilised in up to 40 mL Soluene-350™ (PerkinElmer), and the cotton swabs and surgical gauze used to remove residual SM or WoundStat™ from the treatment site were placed into isopropanol (20 mL). Vials were stored at ambient temperature for at least 14 days (with occasional vigorous shaking) to allow dissolution and extraction into the respective solvent. Radioactivity within the samples was quantified (disintegrations per minute) by liquid scintillation counting (Model 2810 Tri-Carb, PerkinElmer). Standard solutions containing known amounts of ^{14}C-SM were prepared in triplicate for cotton swabs, surgical gauze, WoundStat™ and skin, using the same method as for the experimental samples. Aliquots (250 µL) of standards and experimental samples were diluted in a 5 mL Ultima Gold™ liquid scintillation cocktail (PerkinElmer) for analysis. Blood samples were colour-bleached to reduce quenching, using previously described methods (Moore, 1981). Briefly, triplicate aliquots of blood (0.4 mL) were solubilised in 1 mL Soluene-350™ and isopropanol solution in a 1:2 ratio and incubated at 60°C for 2 h. Samples were cooled and incubated with hydrogen peroxide solution (0.5 mL; 30% v/v) for 30 min at ambient temperature. Blood samples were subsequently incubated at 60°C for 30 min. Triplicate organ samples (100 mg) were solubilised in Soluene-350™ (2 mL) with a 4 h incubation period at 60°C. Both blood and organ samples were cooled and diluted in a 20 mL Ultima Gold™ liquid scintillation cocktail.

Blood and organ samples for reference standards were obtained from non-exposed animals. Standard solutions containing known amounts of ^{14}C-SM were prepared in triplicate following the methods described above. To account for differences in weight/volume ratio among the organ samples the densities were determined using homogenised samples. Densities for organ samples were as follows; brain (0.87 g mL^{-1}), heart (0.89 g mL^{-1}), lungs (0.77 g mL^{-1}), liver (0.98 g mL^{-1}), spleen (0.96 g mL^{-1}), pancreas (0.84 g mL^{-1}), kidney (0.91 g mL^{-1}) and small intestine (0.89 g mL^{-1}).

Both experimental samples and reference standards were analysed by liquid scintillation counting, using a 2 min count time, with the exception of the organ and blood samples, which used a 5 min count time. Pre-set quench settings were used for the Ultima Gold™ liquid scintillation cocktail. The quantity of radioactivity in each sample was converted to a measure of ^{14}C-radiolabelled SM by comparison with the corresponding reference standards (measured simultaneously). Radiolabel (^{14}C) elimination kinetics for the blood were calculated from linear regression analysis of a semi-logarithmic plot of blood concentration against time at steady state, where the decrease in concentration of ^{14}C-SM with time was constant. Area under the curve (AUC), t_{max} and C_{max} were calculated by non-compartmental analysis using GraphPad Prism version 6.01 for Windows (GraphPad Software).

Histological analysis

Full-thickness skin biopsies were collected from each treatment site *post mortem* and immediately fixed in 10% neutral buffered formalin. Fixed skin samples were processed through graded ethanol series and cleared prior to being infiltrated and embedded in paraffin wax. Wax-embedded blocks were sectioned at a nominal thickness of 5 µm and stained with haematoxylin and eosin. Stained skin sections were examined by a qualified histopathologist. Each section was subjectively scored for the occurrence and severity of several indicators, including keratinocyte necrosis,

eschar formation, sub-epidermal separation or vesication, blood vessel dilation, and inflammatory cell infiltrate.

Statistical analysis

For each parameter, the mean and standard deviation (SD) were calculated for each treatment site at each time point. Data from the untreated control skin sites and the damaged unexposed skin sites were pooled (separately) for the two groups of animals (SM control and WoundStat™ decontamination treatment groups) to facilitate graphical representation of the results. GraphPad Prism version 6.01 for Windows (GraphPad Software) was used for normality testing and statistical analysis of the data. Data were assessed for normal distribution using a D'Agostino and Pearson omnibus normality test and a Gaussian non-linear regression curve fit. Significance was predefined at an alpha-level of 0.05.

One-way analysis of variance (ANOVA) with Bonferroni's multiple comparisons post test was used for inter-group comparisons of normally distributed data. Student's t-test was used to analyse differences between two normally distributed groups. For data that did not fit a Gaussian distribution, Kruskal–Wallis one-way ANOVA with Dunn's post test was used to analyse multiple inter-group comparisons. Comparisons between two groups involving data that did not meet normal distribution criteria were analysed using a two-tailed Mann–Whitney U test.

Results

Gross clinical observations

Exposure of damaged skin to SM resulted in skin blanching at the treatment site within 60 min for all animals in the SM control group. All animals in this group also developed an ulcerated area or skin erosion directly below the SM droplet within 6 hours, as evidenced by a pale area of skin with a "peau d'orange" appearance. In the WoundStat™ decontamination group, observable skin blanching was reduced by two thirds (2 out of 6 animals) and no ulcerated area developed in any of the 6 animals.

Treatment with WoundStat™ did not significantly change the frequency (n=4/6 animals) or time to the appearance of erythema, with the median time to observable erythema being 120 min for both treated and untreated sites. Decontamination with WoundStat™ both reduced the frequency of oedema at the exposure site (n=2/6 animals in WoundStat™ decontamination group), and prolonged the latency period between the SM challenge and the appearance of oedema compared to the SM control group (180 min vs. 100 min, respectively).

Overall there were no remarkable visual changes seen over the 6-hour study period for the control (undamaged skin) site and damaged skin site for either group of animals. Additionally, application of WoundStat™ did not appear to adversely affect damaged skin, as there was no notable difference in appearance between the treated and untreated sites that had not been exposed to SM.

Microscopic skin structure changes

Histological examination confirmed that dermatoming achieved complete removal of the SC and epidermis (Figure 1). The remaining intact epithelium (at the

edge of the treatment site) was histologically normal, as were the hair follicles and other adnexal structures. All control (undamaged) skin slides appeared normal for both treatment groups.

There were no significant microscopic differences between the damaged and SM skin sites for animals in the SM control group (Table 1). Additionally, there were no significant microscopic differences between SM-exposed sites with and without decontamination using WoundStat™ (Table 1). Both groups showed mild, perivascular, polymorphonuclear neutrophil (PMN) infiltrate in the dermis (Figure 1), as well as increased PMNs within the capillary lumen (Table 1). These findings were consistent with secondary tissue damage caused by the dermatome, which was observed at the damaged unexposed skin sites in both SM control and WoundStat™ decontamination groups.

Biophysical measurements

Cutaneous blood flow (laser Doppler imaging)

Overall, blood flow increased at the treatment sites during the 6 h study period (Figures 2 and 3). However, exposure to SM significantly reduced skin blood flow compared to unexposed damaged skin sites from 180 min post-exposure until the study end at 6 h post exposure (Figure 2), with a distinct area of low flux observed at the site of the SM application (Figure 3). Decontamination with WoundStat™ prevented this significant decrease in blood flow at all time points except 120 min post-exposure (Figure 2). Furthermore, the distinct area of low flux observed at the SM treatment site following SM exposure was not observed at sites treated with WoundStat™ (Figure 3).

Skin barrier integrity (transepidermal water loss)

Overall, removal of the SC and epidermis, regardless of any additional intervention (WoundStat™ and/or SM), resulted in a statistically significant increase in TEWL compared to control (undamaged) skin sites. No statistically significant difference was observed between WoundStat™ treated skin with or without prior SM-exposure (Figure 4). However, sites treated with WoundStat™ had significantly higher TEWL values compared to untreated damaged skin sites and SM-exposed sites at 120 min post-exposure (Figure 4). Additionally, SM sites treated with WoundStat™ showed significantly greater TEWL values compared to SM treatment sites at 60, 180 and 240 min post exposure (Figure 4).

Skin colour (skin reflectance spectroscopy)

Removal of the upper skin layers significantly decreased skin brightness (L* CIELAB parameter) and significantly increased skin redness (a* CIELAB parameter) and skin hue or yellowness (b* CIELAB parameter) compared to undamaged skin sites ($P<0.01$; data not shown). However, treatment with WoundStat™ was not associated with a significant difference in any of the skin colour parameters measured at SM-exposed sites. Exposure to SM without decontamination using WoundStat™ resulted in a distinct trough at ~420 nm in the skin reflectance spectra at 6 h post-exposure, when data were expressed as a percentage change from baseline values; this was not observed at any other skin sites (Figure 5). Conversely, skin reflectance between ~450–600 nm was greater at SM-exposed sites treated with WoundStat™ than at all other sites.

Skin surface temperature (infrared thermography)

Damage to the skin (removal of the SC and epidermis) resulted in a significant decrease in skin surface temperature (data not shown). However, no significant difference in skin surface temperature was observed between any of the damaged skin treatment sites (data not shown).

Toxicokinetics

Blood concentrations of ^{14}C-SM peaked at 120 min post-challenge for both SM control and WoundStat™ decontamination groups (Figure 6). However, WoundStat™ treatment post-exposure significantly reduced the amount of ^{14}C-SM measured in the blood at all time points (42–50% reduction; Figure 6). Elimination kinetics parameters, including peak concentration, slope and elimination constant, were derived from a semi-logarithmic plot of the ^{14}C-SM blood concentrations, as shown in Figure 6. These parameters were significantly decreased, whilst the apparent volume of distribution was significantly increased for animals in the WoundStat™ decontamination group compared to those in the SM control group ($P<0.01$, Figure 6). However, there was no significant difference in either the apparent half-life of ^{14}C-SM or the SM dose (calculated from the apparent volume of distribution and C_{max}) between the two groups (Figure 6).

Distribution of 14C-sulphur mustard

Overall, 6.3 ± 1.6% of the applied dose of ^{14}C-SM was recovered from samples taken from animals in the SM control group, including exposure site skin, skin surface swabs, organs and blood. The skin surface swabs and exposure site skin accounted for the largest proportion of ^{14}C-SM recovered. Use of WoundStat™ as a decontaminant significantly reduced the amount of ^{14}C-SM recovered from the skin (85 ± 16 µg vs. 279 ± 24 µg) and skin surface swabs (4 ± 1 µg vs. 440 ± 82 µg) compared to animals in the SM control group (Figure 7). The ^{14}C-SM recovered from WoundStat™ accounted for the majority (99 ± 8%) of the recovered ^{14}C-SM dose for animals in the WoundStat™ decontamination group (Figure 7).

Despite the significant decrease in the amount of ^{14}C-SM absorbed following WoundStat™ decontamination compared to the SM control group, the amount of ^{14}C-SM in the organ samples was very similar in both groups (Figure 8). In both groups, when the data were expressed as ng of ^{14}C-SM per g of organ weight, the predominant distribution of ^{14}C-SM in the organs was the same: primarily the kidney, followed by the liver and small intestine (Figure 8). However, there were significant differences between the SM control and WoundStat™ decontamination groups in the amount of ^{14}C-SM recovered from the liver samples (Figure 8).

Discussion

This study has demonstrated that removal of the skin barrier layer (SC and epidermis) resulted in the rapid onset of advanced signs of SM toxicity, including ulceration, eschar formation and reduced dermal blood flow, with a shorter latency period compared to that of undamaged skin exposed to the same amount of SM (Larner, unpublished observations). The latency period between exposure and advanced signs of SM toxicity was also shorter than that reported in studies conducted by Reid and colleagues, in which both the amount of SM applied to the skin (400 µL) and the exposure duration (2 h) were greater than those used in this

study (Reid *et al*., 2000). The rapid appearance of these advanced signs of toxicity correlated with an increased rate of absorption *in vivo* and these data are in agreement with *in vitro* percutaneous penetration studies (Lydon *et al*., 2017). This suggests that the latency period between SM exposure and the appearance of symptoms in undamaged skin could be in part due to delayed absorption and not, as previously hypothesised, exclusively by cellular processes such as DNA damage or inflammatory-mediated responses (Arroyo *et al*., 2000; Papirmeister *et al*., 1985). The rapid onset of symptoms of severe toxicity associated with the exposure of barrier-compromised skin to SM may potentially reduce the window of opportunity for successful therapeutic interventions. However, application of WoundStat™ to the exposure site prevented or delayed signs of toxicity, including ulceration; thus, the use of WoundStat™ as a decontaminant may reduce lesion severity and increase the time interval during which additional therapeutic interventions may be effective.

To our knowledge, this study is the first to examine the toxicokinetics and distribution of ^{14}C-SM when applied percutaneously to superficially damaged skin. Absorption of ^{14}C-SM into the circulation was rapid, and the toxicokinetics of ^{14}C-SM in the blood followed a first-order non-compartmental model with an apparent half-life of 460 ± 62 min. SM has been found to form a skin reservoir within the SC *in vitro* (Hattersley *et al*., 2008), although it is not clear whether any reservoir of active SM forms in the dermis if the SC is removed. However, SM rapidly spreads across the surface of human skin *in vitro* (Chilcott *et al*., 2000) and so could form a reservoir in the SC in the undamaged skin surrounding the area of damaged skin. Total recovery of ^{14}C-SM from the skin, skin surface swabs, blood and internal organ samples in the SM control group was congruent with the percentage dose penetration in an *ex vivo* isolated perfused porcine skin flap model at a comparable time-point (Riviere *et al*., 1995). For animals in the SM control group, the largest proportion of ^{14}C-SM was recovered from the skin surface swabs and the skin at the exposure site. Once absorbed, the majority of the ^{14}C resided within either the skin or blood, which is in agreement with previous studies (Hambrook *et al*., 1992). Application of WoundStat™ significantly reduced the amount of ^{14}C-SM recovered from both skin surface swabs and skin at the exposure site compared to the SM control group ($P<0.001$), with the majority of the ^{14}C-SM dose being sequestered in the retained WoundStat™.

The distribution of radioactivity within internal organs is in agreement with studies in the literature (Black *et al*., 1992; Davison *et al*., 1961; Hambrook *et al*., 1992; Maisonneuve *et al*., 1993). Decontamination with WoundStat™ significantly reduced the amount of ^{14}C-SM detected in the liver, presumably by inhibiting the dermal absorption of SM. However, the use of liquid scintillation counting to quantify ^{14}C-SM does not allow for speciation of the ^{14}C-radiolabel isotope. Metabolite identification was not the primary focus of this work, but it has previously been shown that SM is conjugated or hydrolysed *in vivo* (Black *et al*., 1992; Capacio *et al*., 2004). Thus, the smaller amount of ^{14}C isotope measured in the liver could be attributed to changes in the concentration of hydrolysis or conjugation products as a result of an altered SM metabolism (Black *et al*., 1992; Black and Read, 1995), rather than just a reduction in systemic absorption. Speciation of radiolabelled compounds using previously characterised techniques (Noort *et al*., 2008, 1999) would enable the identification of the SM parent molecule or metabolites and conjugates within samples.

The biophysical methods used in this study enable a non-invasive and quantitative assessment of SM injuries, offering considerable ethical refinement and

reducing the number of animals required. These methods permit sequential measurements under terminal anaesthesia over a shorter time frame, whereas SM injuries would previously have been assessed visually or by histopathology, typically 14 to 21 days post-exposure.

This study has built on previous work in demonstrating the usefulness of laser Doppler imaging (LDI) in measuring SM lesion progression (Braue *et al*., 2007; Brown *et al*., 1998; Chilcott *et al*., 2000). All animals in the SM control group rapidly developed (within 60 min of exposure) an area of blanched skin surrounding the SM droplet, which correlated with a foci of reduced maximal blood flow, as measured by LDI. Histopathological analysis revealed capillary dilation and congestion of subepidermal capillaries with perivascular inflammatory cell infiltrate, consistent with other published studies that also reported significantly reduced skin blood flow at the lesion site (Brown *et al*., 1998; Brown and Rice, 1997). Whilst a transient decrease in perfusion units was seen following WoundStat™ decontamination of SM-exposed skin (compared to WoundStat™-treated unexposed skin), sustained foci of reduced blood flow were not observed. Moreover, the frequency of visual blanching at the exposure site also decreased following decontamination with WoundStat™.

In contrast, this study has highlighted that some other commonly used biophysical measurements (skin reflectance spectroscopy, infrared thermography and TEWL water loss) may have limited value when investigating the response of damaged skin to SM, as initial pathological changes could be masked by the mechanical damage caused by dermatoming. Removal of the SC and epidermis resulted in statistically significant increases in both skin redness (a*) and hue (b*). The increase in these two parameters can be attributed to punctate haemorrhage and inflammation (increased a* or skin redness) and sero-cellular crusting or eschar formation (increased b* or skin yellowness) following the removal of the upper skin layers. In contrast with previous studies, SM did not have a significant effect on skin colour in terms of CIELAB L*a*b* parameters compared to the appropriate control site (Chilcott *et al*., 2000). Similarly, there was no significant difference in the colour parameters measured (L*, a* and b*) between the SM control and the WoundStat™ decontamination treatment groups. This was unexpected, as erythema at the exposure site was visible in half the animals at 2 hours post challenge. However, removal of the upper skin layers resulted in the unexposed skin becoming erythematous. Therefore, although a qualitative difference in skin redness was observed between the SM-exposed and unexposed skin it was not deemed statistically significant in terms of the a* value.

Despite the lack of SM-dependent effects on CIELAB colour values there were overt changes in the skin reflectance spectra between the treatment groups. Most notable was the increase in skin absorbance at ~420 nm at 6 h post-exposure for the SM-only site. Such changes in the absorption spectra may be attributed to an increase in bilirubin levels (Anderson and Parrish, 1981) which has previously been reported following SM exposure in humans (Pourfarzam *et al*., 2009). Increased bilirubin could be a direct result of toxic effects of SM on the liver. The hepatic metabolism of SM has been reported in the literature (Black and Read, 1995; Halme *et al*., 2015; Jafari, 2007) and radiometric data from this study provide further evidence that ^{14}C-SM or radiolabelled metabolites of SM are associated with the liver. Furthermore, decontamination with WoundStat™ significantly decreased the amount of radiolabelled ^{14}C detected in the liver, which is consistent with the absence of increased skin absorption at ~420 nm in this group. Alternatively, bilirubin, like glutathione (GSH), has been shown to have an antioxidant and

cytoprotective role (Sedlak *et al*., 2009). Whilst GSH primarily protects hydrophilic proteins, bilirubin is lipophilic and prevents oxidative damage to lipids and lipophilic proteins (Sedlak *et al*., 2009). GSH has a well-established role in cellular defence and depletion of GSH levels is associated with SM toxicity (Jafari, 2007), whereas administration of exogenous GSH has been shown to be protective *in vitro* and in animal models (Tewari-Singh *et al*., 2011). Thus, bilirubin may act as an antioxidant in lipophilic environments such as the skin and so act as a defence mechanism against SM-associated lipid peroxidation.

Unsurprisingly, removal of the skin barrier (loss of SC and epidermis) with a dermatome resulted in significantly increased TEWL rates compared to undamaged control values. However, over the 6-hour study period no significant differences were observed for damaged skin sites with and without SM-exposure in the SM control group. Presumably this is because the key factor associated with increased evaporative water loss in this model is the complete removal of the barrier layer. Thus, any additional changes associated with SM exposure were not evident up to 6 h post-exposure, which is consistent with findings from previous studies using undamaged skin porcine models (Chilcott *et al*., 2000). Moreover, the application of WoundStat™ to damaged skin resulted in significantly greater TEWL values compared to other damaged skin sites (±SM exposure). The phenomenon of increased TEWL in response to the application of semi-occlusive dressings has been previously reported (Schunck *et al*., 2005). Therefore, whilst WoundStat™ is *in situ* it may act as a barrier to TEWL and so prevent the normal increased TEWL feedback mechanism associated with complete barrier loss. This may conceivably prevent the stimulation of parakeratosis and other related barrier mechanisms, which are normally rapidly activated in open wounds to prevent the ingress of harmful substances or bacteria (Schunck *et al*., 2005).

Exposure of damaged skin to SM did not result in any significant microscopic differences compared to either unexposed damaged skin or skin at WoundStat™ decontaminated sites. This was unexpected, given the significant differences in both blood flow and the amount of ^{14}C-SM retained within the skin at WoundStat™ decontaminated sites compared to sites not receiving decontamination. However, the presence of a few definite structural alterations at 6 hours post exposure is in agreement with previous SM studies using undamaged skin study (Brown and Rice, 1997; Greenberg *et al*., 2006), although these studies observed SM-associated focal vacuolation and pyknotic nuclei in basal keratinocytes, which were not observed in the present study. It is likely that the removal of the epidermis and the associated acute inflammatory response resulting from the initial tissue damage may mask any additional histopathological changes caused by SM at this early time point. With that in mind, one concern with using skin sites from the same animal as a control was the induction of a systemic inflammatory response to SM that could affect the surrounding dorsal skin. However, no significant microscopic changes in the gross skin structure at undamaged control skin sites were observed in either the SM control or WoundStat™ decontamination groups.

Conclusions

Direct application of SM to superficial wounds results in the rapid appearance of advanced signs of toxicity, such as ulceration and reduced blood flow, and may increase the urgency for the effective decontamination of SM-contaminated wounds. In addition, there is evidence to suggest that the latent period between SM exposure

and the appearance of symptoms may be attributed in part to delayed absorption and not exclusively to cellular processes, as previously described. Moreover, this study has built upon the previous evidence base describing the usefulness of LDI for monitoring SM injuries and highlights the limitations of commonly used biophysical measurements (SRS, infrared thermography and TEWL) when monitoring SM injuries on damaged skin. This study also demonstrates that the timely application of WoundStat™ can prevent advanced signs of SM dermal toxicity, namely ulceration, improve blood flow at the exposure site, and significantly reduce the amount of ^{14}C-SM recovered from the blood, skin and liver.

REFERENCES

Anderson RR, Parrish JA. 1981. The optics of human skin. *J. Invest. Dermatol.* **77**: 13–19.

Arroyo CM, Schafer RJ, Kurt EM, Broomfield CA, Carmichael AJ. 2000. Response of normal human keratinocytes to sulfur mustard: cytokine release. *J. Appl. Toxicol.* **20 Suppl 1**: S63–72.

Black RM, Hambrook JL, Howells DJ, Read RW. 1992. Biological fate of sulfur mustard, 1,1'-thiobis(2-chloroethane). Urinary excretion profiles of hydrolysis products and beta-lyase metabolites of sulfur mustard after cutaneous application in rats. *J. Anal. Toxicol.* **16**: 79–84.

Black RM, Read RW. 1995. Biological fate of sulphur mustard, 1,1'-thiobis(2-chloroethane): identification of beta-lyase metabolites and hydrolysis products in human urine. *Xenobiotica* **25**: 167–173. DOI:10.3109/00498259509061842.

Braue EH Jr, Graham JS, Doxzon BF, Hanssen KA, Lumpkin HL, Stevenson RS, Deckert RR, Dalal SJ, Mitcheltree LW. 2007. Noninvasive methods for determining lesion depth from vesicant exposure. *J. Burn. Care. Res.* **28**: 275–285. DOI:10.1097/BCR.0B013E318031A1A8.

Brown RF, Rice P. 1997. Histopathological changes in Yucatan minipig skin following challenge with sulphur mustard. A sequential study of the first 24 hours following challenge. *Int. J. Exp. Pathol.* **78**: 9–20.

Brown RF, Rice P, Bennett NJ. 1998. The use of laser Doppler imaging as an aid in clinical management decision making in the treatment of vesicant burns. *Burns* **24**: 692–698.

Capacio BR, Smith JR, DeLion MT, Anderson DR, Graham JS, Platoff GE, Korte WD. 2004. Monitoring sulfur mustard exposure by gas chromatography-mass spectrometry analysis of thiodiglycol cleaved from blood proteins. *J. Anal. Toxicol.* **28**: 306–310.

Chilcott RP, Brown RF, Rice P. 2000. Non-invasive quantification of skin injury resulting from exposure to sulphur mustard and Lewisite vapours. *Burns* **26**: 245–250. DOI:10.1016/S0305-4179(99)00129-1.

Chilcott RP, Dalton CH, Ashley Z, Allen CE, Bradley ST, Maidment MP, Jenner J, Brown RF, Gwyther RJ, Rice P. 2007. Evaluation of barrier creams against sulphur mustard: (II) In vivo and in vitro studies using the domestic white pig. *Cutan. Ocul. Toxicol.* **26**: 235–247. DOI:10.1080/15569520701212373.

Chilcott RP, Jenner J, Carrick W, Hotchkiss SA, Rice P. 2000. Human skin absorption of Bis-2-(chloroethyl)sulphide (sulphur mustard) in vitro. *J. Appl. Toxicol.* **20**: 349–355. DOI:10.1002/1099-1263(200009/10)20:5<349::AID-JAT713>3.0.CO;2-O.

Dalton CH, Hall CA, Lydon HL, Chipman JK, Graham JS, Jenner J, Chilcott RP. 2015. Development of haemostatic decontaminants for the treatment of wounds contaminated with chemical warfare agents. 2: evaluation of in vitro topical decontamination efficacy using undamaged skin. *J. Appl. Toxicol.* **35**: 543–550. DOI:10.1002/jat.3060.

Davison C, Rozman RS, Smith PK. 1961. Metabolism of bis-beta-chloroethyl sulfide (sulfur mustard gas). *Biochem. Pharmacol.* **7**: 65–74.

Gibbs AR, Pooley FD. 1994. Fuller's earth (montmorillonite) pneumoconiosis. *Occup. Environ. Med.* **51**: 644–646.

Gold MB, Bongiovanni R, Scharf BA, Gresham VC, Woodward CL. 1994. Hypochlorite solution as a decontaminant in sulfur mustard contaminated skin defects in the euthymic hairless guinea pig. *Drug. Chem. Toxicol.* **17**: 499–527. DOI:10.3109/01480549409014314.

Graham, JS, Chilcott, RP, Rice, P, Milner, SM, Hurst, CG, Maliner, BI, 2005. Wound healing of cutaneous sulfur mustard injuries: strategies for the development of improved therapies. *J Burns Wounds* **4**, e1.

Graham JS, Martin JL, Zallnick JE, Nalls CR, Mitcheltree LW, Lee RB, Logan TP, Braue EH, 1999. Assessment of cutaneous sulfur mustard injury in the weanling pig. *Skin Res. Technol*. **5**, 56–67. DOI:10.1111/j.1600-0846.1999.tb00206.x.

Graham JS, Reid FM, Smith JR, Stotts RR, Tucker ES, Shumaker SM, Niemuth NA, Janny SJ. 2000. A cutaneous full-thickness liquid sulfur mustard burn model in weanling swine: clinical pathology and urinary excretion of thiodiglycol. *J. Appl. Toxicol.* **20 Suppl 1**: S161–172.

Greenberg S, Kamath P, Petrali J, Hamilton T, Garfield J, Garlick JA. 2006. Characterization of the initial response of engineered human skin to sulfur mustard. *Toxicol. Sci.* **90**: 549–557. DOI:10.1093/toxsci/kfi306.

Hall CA, Lydon HL, Dalton CH, Chipman JK, Graham JS, Chilcott RP. 2015. Development of haemostatic decontaminants for the treatment of wounds contaminated with chemical warfare agents. 1: evaluation of in vitro clotting efficacy in the presence of certain contaminants. *J. Appl. Toxicol.* **35**: 536–542. DOI:10.1002/jat.3019.

Halme M, Pesonen M, Hakala U, Pasanen M, Vähäkangas K, Vanninen P. 2015. Applying human and pig hepatic in vitro experiments for sulfur mustard study: screening and identification of metabolites by liquid chromatography/tandem mass spectrometry. *Rapid Commun. Mass. Spectrom.* **29**: 1279–1287. DOI:10.1002/rcm.7218.

Hambrook JL, Harrison JM, Howells DJ, Schock C. 1992. Biological fate of sulphur mustard (1,1'-thio-bis(2-chloroethane)): urinary and faecal excretion of 35S by rat after injection or cutaneous application of 35S-labelled sulphur mustard. *Xenobiotica* **22**: 65–75.

Hattersley IJ, Jenner J, Dalton C, Chilcott RP, Graham JS. 2008. The skin reservoir of sulphur mustard. *Toxicol. In Vitro* **22**: 1539–1546. DOI:10.1016/j.tiv.2008.06.002.

Ireland, M.W., 1926. Medical aspects of gas warfare. U.S. Governm. Print. Off, Washington.

Jafari M. 2007. Dose- and time-dependent effects of sulfur mustard on antioxidant system in liver and brain of rat. *Toxicology* **231**: 30–39. DOI:10.1016/j.tox.2006.11.048.

Jenner J, Graham SJ. 2013. Treatment of sulphur mustard skin injury. *Chem. Biol. Interact.* **206**: 491–495. DOI:10.1016/j.cbi.2013.10.015.

Kehe K, Szinicz L. 2005. Medical aspects of sulphur mustard poisoning. *Toxicology* **214**: 198–209. DOI:10.1016/j.tox.2005.06.014.

Lydon HL, Hall CA, Dalton CH, Chipman JK, Graham JS, Chilcott RP. Development of haemostatic decontaminants for treatment of wounds contaminated with chemical warfare agents. 3: Evaluation of in vitro topical decontamination efficacy using damaged skin. *J. Appl. Toxicol.* 2017. In press. DOI:10.1002/jat.3446

Maisonneuve A, Callebat I, Debordes L, Coppet L. 1993. Biological fate of sulphur mustard in rat: toxicokinetics and disposition. *Xenobiotica* **23**: 771–780.

Mitcheltree LW, Mershon MM, Wall HG, Pulliam JD, Manthei JH, 1989. Microblister Formation in Vesicant-Exposed Pig Skin. *J. Toxicol. Cutaneous Ocul. Toxicol.* **8**, 309–319. DOI:10.3109/15569528909062934.

Monteiro-Riviere NA, Inman AO. 1997. Ultrastructural characterization of sulfur mustard-induced vesication in isolated perfused porcine skin. *Microsc. Res. Tech.* **37**: 229–241. DOI**:**10.1002/(SICI)1097-0029(19970501)37:3<229::AID-JEMT8>3.0.CO;2-I

Moore PA. 1981. Preparation of whole blood for liquid scintillation counting. *Clin. Chem.* **27**: 609–611.

Noort D, Fidder A, Degenhardt-Langelaan CE, Hulst AG. 2008. Retrospective detection of sulfur mustard exposure by mass spectrometric analysis of adducts to albumin and hemoglobin: an in vivo study. *J. Anal. Toxicol.* **32**: 25–30.

Noort D, Hulst AG, de Jong LP, Benschop HP. 1999. Alkylation of human serum albumin by sulfur mustard in vitro and in vivo: mass spectrometric analysis of a cysteine adduct as a sensitive biomarker of exposure. *Chem. Res. Toxicol.* **12**: 715–721. DOI:10.1021/tx9900369.

Papirmeister B, Gross CL, Meier HL, Petrali JP, Johnson JB. 1985. Molecular basis for mustard-induced vesication. *Fundam. Appl. Toxicol.* **5**: S134–149.

Petrali JP, Oglesby-Megee S. 1997. Toxicity of Mustard Gas Skin Lesions. *Microsc. Res. Tech.* **37**: 221–228. DOI:10.1002/(SICI)1097-0029(19970501)37:3<221::AID-JEMT7>3.0.CO;2-Q

Pourfarzam S, Ghazanfari T, Merasizadeh J, Ghanei M, Azimi G, Araghizadeh H, Foroutan A, Shams J, Ghasemi H, Yaraee R, Shariat-Panahi S, Soroush MR, Hassan ZM, Moaiedmohseni S, Nadoushan MRJ, Fallahi F, Mahdavi MRV, Moin A, Ghazanfari Z, Ghaderi S, Yarmohammadi ME, Naghizadeh MM, Faghihzadeh S, 2009. Long-term pulmonary complications in sulfur mustard victims of Sardasht, *Iran Toxin. Reviews* **28**, 8–13. DOI:10.1080/15569540802689220.

Price JA, Rogers JV, McDougal JN, Shaw MQ, Reid FM, Graham JS. 2009. Transcriptional changes in porcine skin at 7 days following sulfur mustard and thermal burn injury. *Cutan. Ocul. Toxicol.* **28**: 129–140. DOI:10.1080/15569520903097754.

Reid FM, Graham J, Niemuth NA, Singer AW, Janny SJ, Johnson JB. 2000. Sulfur mustard-induced skin burns in weanling swine evaluated clinically and histopathologically. *J. Appl. Toxicol.* **20 Suppl 1**: S153–160.

Rice P, 2016. Sulphur mustard. *Medicine* **44**, 111–112. DOI:10.1016/j.mpmed.2015.11.010.

Rice P. 2003. Sulphur mustard injuries of the skin. Pathophysiology and management. *Toxicol. Rev.* **22**: 111–118.

Riviere JE, Brooks JD, Williams PL, Monteiro-Riviere NA. 1995. Toxicokinetics of topical sulfur mustard penetration, disposition, and vascular toxicity in isolated perfused porcine skin. *Toxicol. Appl. Pharmacol.* **135**: 25–34.

Schunck M, Neumann C, Proksch E. 2005. Artificial barrier repair in wounds by semi-occlusive foils reduced wound contraction and enhanced cell migration and reepithelization in mouse skin. *J. Invest. Dermatol.* **125**: 1063–1071. DOI:10.1111/j.0022-202X.2005.23890.x.

Sedlak TW, Saleh M, Higginson DS, Paul BD, Juluri KR, Snyder SH, 2009. Bilirubin and glutathione have complementary antioxidant and cytoprotective roles. *Proc. Natl. Acad. Sci. U S A.* **106**, 5171–5176.

Smith KJ, Casillas R, Graham J, Skelton HG, Stemler F, Hackley BE Jr. 1997. Histopathologic features seen with different animal models following cutaneous sulfur mustard exposure. *J. Dermatol. Sci.* **14**: 126–135.

Taysse L, Daulon S, Delamanche S, Bellier B, Breton P. 2007. Skin decontamination of mustards and organophosphates: comparative efficiency of RSDL and Fuller's earth in domestic swine. *Hum. Exp. Toxicol.* **26**: 135–141.

Taysse L, Dorandeu F, Daulon S, Foquin A, Perrier N, Lallement G, Breton P. 2011. Cutaneous challenge with chemical warfare agents in the SKH-1 hairless mouse (II): effects of some currently used skin decontaminants (RSDL and Fuller's earth) against liquid sulphur mustard and VX exposure. *Hum. Exp. Toxicol.* **30**: 491–498. DOI:10.1177/0960327110373616.

Tewari-Singh N, Agarwal C, Huang J, Day BJ, White CW, Agarwal R. 2011. Efficacy of glutathione in ameliorating sulfur mustard analog-induced toxicity in cultured skin epidermal cells and in SKH-1 mouse skin in vivo. *J. Pharmacol. Exp. Ther.* **336**: 450–459. DOI:10.1124/jpet.110.173708.

Vogt RF Jr, Dannenberg AM Jr, Schofield BH, Hynes NA, Papirmeister B. 1984. Pathogenesis of skin lesions caused by sulfur mustard. *Fundam. Appl. Toxicol*. **4(2 Pt 2)**: S71-83.

Walters TJ, Kauvar DS, Reeder J, Baer DG. 2007. Effect of reactive skin decontamination lotion on skin wound healing in laboratory rats. *Mil. Med.* **172**: 318–321.

Wattana M, Bey T. 2009. Mustard gas or sulfur mustard: an old chemical agent as a new terrorist threat. *Prehosp. Disaster Med*. 2009 **24**: 19–29.

Wormser U, Brodsky B, Sintov A. 2002. Skin toxicokinetics of mustard gas in the guinea pig: effect of hypochlorite and safety aspects. *Arch. Toxicol.* **76**: 517–522. DOI:10.1007/s00204-002-0362-6.

: S71–83.

Figure legends

Figure 1. Structural changes following exposure of superficially damaged porcine skin to ^{14}C-SM and decontamination with WoundStat™. Representative histological sections prepared from SM-exposed, WoundStat™-decontaminated damaged skin 6 h post-exposure. Eschar formation (E) and neutrophilic cell infiltrate (arrows) are shown. Sections were stained with haematoxylin and eosin and viewed by bright-field microscopy. One representative section from the 6 pigs in the treatment group is shown (original magnification ×20).

Figure 2. Maximum blood perfusion at skin treatment site for the SM control (SM) and WoundStat™ decontamination (WS + SM) treatment groups. Damaged unexposed sites (Damaged) provided a negative control. All values are expressed as mean ± SEM (*n*=6). Statistically significant differences were found when both SM control (SM) and WoundStat™ decontamination (WS + SM) treatment groups were compared to the damaged group. *, *** and **** represent P-values of <0.05, <0.001 and <0.0001, respectively.

Figure 3. Representative skin perfusion images (laser Doppler imaging) for the SM control (SM) and WoundStat™ decontamination (WS + SM) treatment groups. Laser Doppler images of skin with and without SM exposure (but no WoundStat™ decontamination are shaded in grey One representative image from 6 pigs/treatment group is shown.

Figure 4. Transepidermal water loss (TEWL) for skin treatment sites in the SM control (SM) and WoundStat™ decontamination (WS + SM) treatment groups. Flux values (g cm^{-2} h^{-1}) were expressed as a percentage of undamaged control sites for each time point. Damaged unexposed (damaged) and damaged WoundStat™-treated (WS) sites served as respective controls All values are expressed as mean ± SD (*n*=6). Statistically significant differences compared to SM (asterisk) or damaged (dollar sign) are indicated where * or $, ** or $$, ***or $$$ and **** or $$$$ represent P-values of <0.05, <0.01, <0.001 or <0.0001, respectively.

Figure 5. Skin reflectance spectra at 6 hours post-exposure for the SM control (SM) and WoundStat™ decontamination (WS + SM) treatment groups. Data are expressed as percentage changes from baseline values taken immediately prior to dosing. Damaged unexposed (damaged) and damaged WoundStat™ treated (WS) sites served as controls. All values are expressed as mean ± SD (*n*=6).

Figure 6. Measured blood concentrations of ^{14}C-SM for SM control (SM) and WoundStat™ decontamination (WS + SM) treatment groups. Individual values are expressed as mean ± SD (*n*=6).

Figure 7. Recovery of ^{14}C-SM from the samples (WoundStat™, skin surface swabs and skin) expressed as quantity of ^{14}C-SM (µg) recovered in the SM control (SM) and WoundStat™ decontamination (WS + SM) treatment groups. All values are mean ± SD (*n*=6). Data are log transformed to enable comparison. Significant differences between the treatment groups (WS + SM vs. SM) are shown, where *** represents a P-value of <0.001.

Figure 8. Recovery of ^{14}C-SM from internal organs expressed as ng (SM) per g (organ weight) for the SM control (SM) and WoundStat™ decontamination (WS + SM) treatment groups. All values are expressed as mean ± SD (*n*=6). Statistically significant differences between the treatment groups (WS + SM vs. SM) are shown, where * represents a P-value of <0.05.

Table 1. Occurrence and severity of histopathological changes in skin following exposure of superficially damaged porcine skin to ^{14}C-SM and/or decontamination with WoundStat™. Representative histological sections prepared from skin taken 6 h post-exposure for unexposed undamaged skin (control), unexposed damaged skin (damaged), unexposed WoundStat™ decontaminated (WS), SM-exposed (SM), and SM-exposed WoundStat™ decontaminated (WS + SM) treatment sites. Lesions were scored histopathologically, on a scale where ***marked > moderate > mild > minimal > normal*** indicate the severity of the lesion. Numbers in brackets indicate the numbers of animals in each severity group.

Lesion	Treatment Group				
	Control (*n*=12)	Damaged (*n*=12)	WS (*n*=6)	SM (*n*=6)	WS + SM (*n*=6)
Surface and follicular keratinocyte necrosis (n)	Normal (12)	Normal (12)	Normal (6)	Normal (6)	Normal (6)
Subepidermal separation	Normal (12)	Normal (12)	Normal (6)	Normal (6)	Normal (6)
Blood vessel dilation	Normal (12)	Normal (4) Minimal (8)	Normal (5) Minimal (1)	Normal (2) Minimal (4)	Normal (6)
Perivascular to diffuse, neutrophilic cell infiltrate	Normal (12)	Mild (12)	Mild (6)	Mild (6)	Mild (6)
Eschar formation	Normal (12)	Mild (2) Moderate (10)	Mild (1) Moderate (5)	Minimal (2) Mild (4)	Mild (2) Moderate (3) Marked (1)

Table 2. Calculated elimination kinetics of ^{14}C-SM for SM control (SM) and WoundStat™ decontamination (WS + SM) treatment groups. Individual values are expressed as mean ± SD (*n*=6). Elimination kinetics are derived from linear regression analysis of a semi-logarithmic plot of whole blood concentration against time. The equations used were described by Shen (2008). Significant differences between the SM and WS + SM treatment groups are shown, where * and ** represent *P*-values of <0.05 and <0.01, respectively

	SM	**WS + SM**
$t_{½}$ (min)	425 ± 60	468 ± 121
C_{max} (ng.mL^{-1})	60.8 ± 64	**33.0 ± 7.4
t_{max} (min)	120 ± 0	90 ± 33
AUC (ng.min.mL^{-1})	17240 ± 1828	**9407 ± 1922
Slope (pg.mL^{-1}.min^{-1})	-64.7 ± 9.0	*-34.4 ± 13.3
K_{el} (pg.mL^{-1}.min^{-1})	149 ± 21	*79.1 ± 30.7
V_d/F (L)	190 ± 22	***371 ± 83
D (mg)	11.5 ± 0.5	11.7 ± 0.3

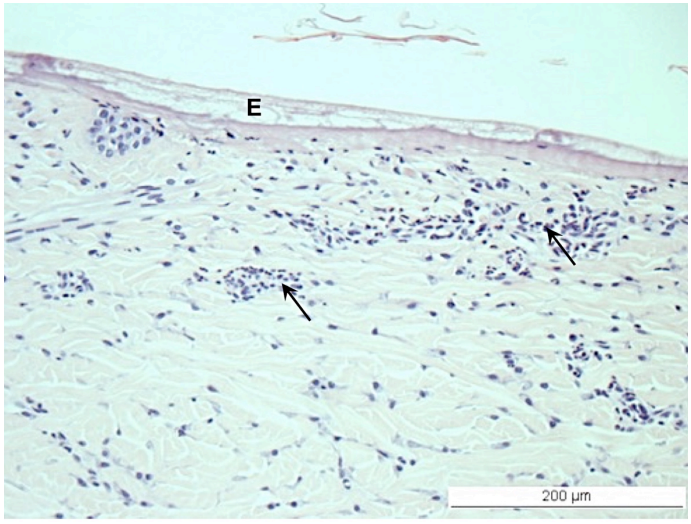

Figure 1

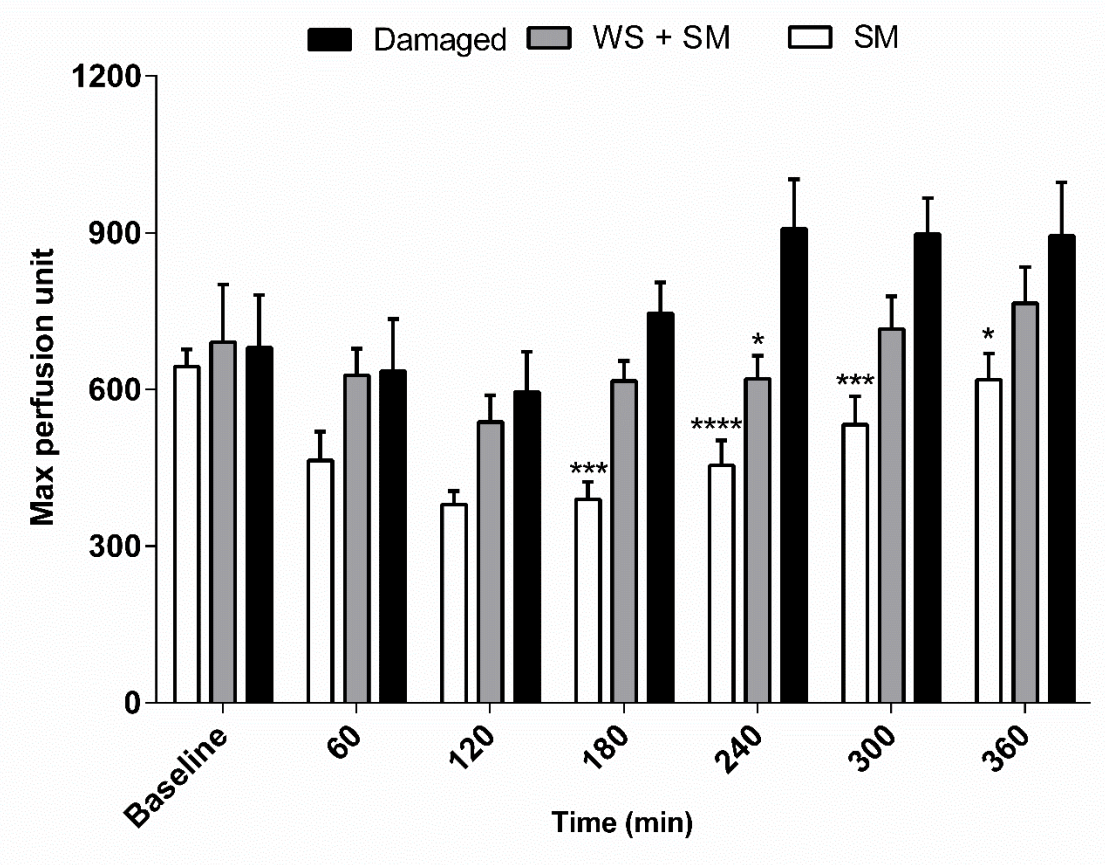
Damaged
WS + SM
SM
1200
900
600
300
0
Max perfusion unit
***
****
*
***
*
Baseline
60
120
180
240
300
360
Time (min)

Figure 2

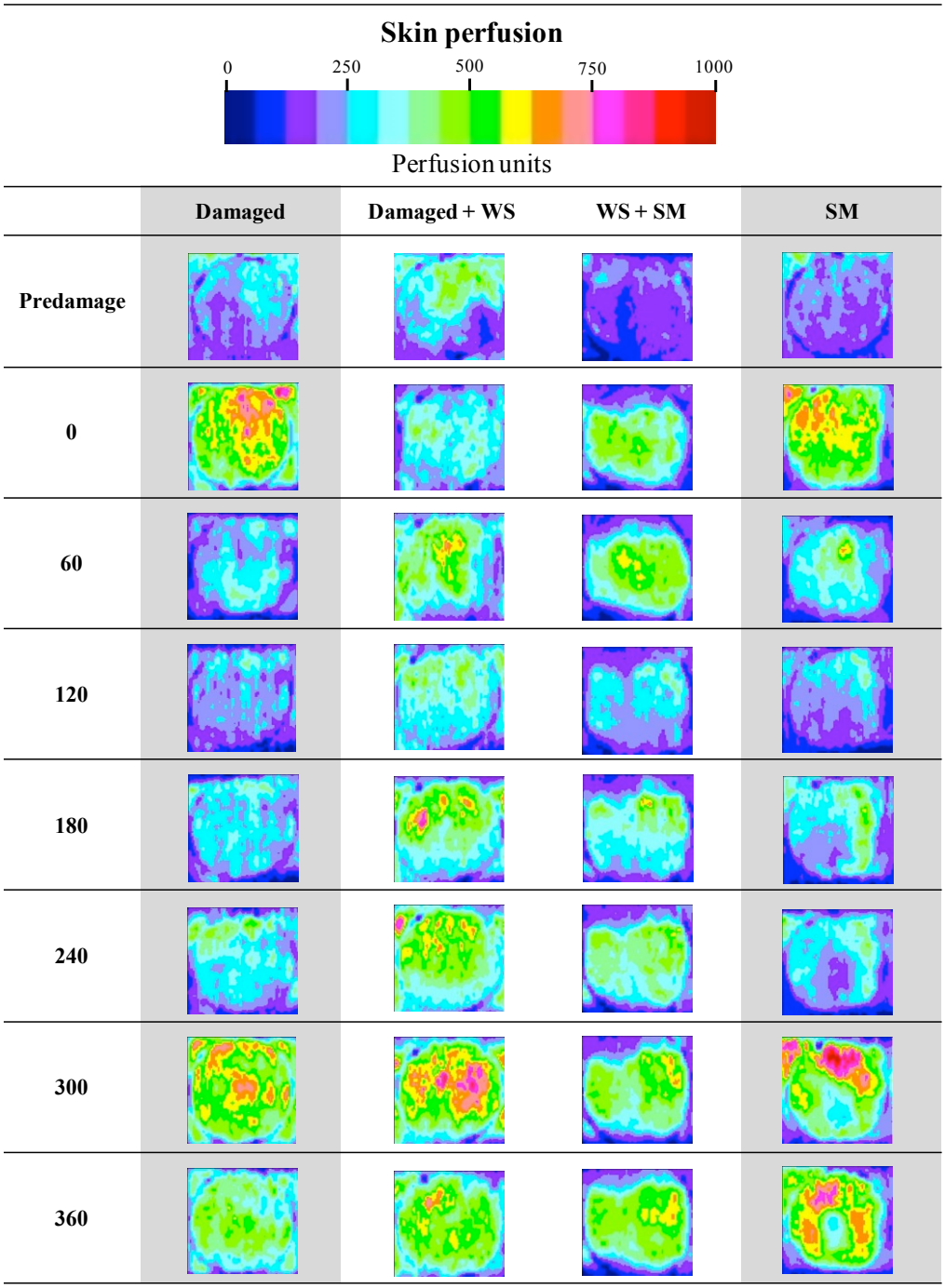
Skin perfusion
0
250
500
750
1000
Perfusion units
Damaged
Damaged + WS
WS + SM
SM
Predamage
0
60
120
180
240
300
360

Figure 3

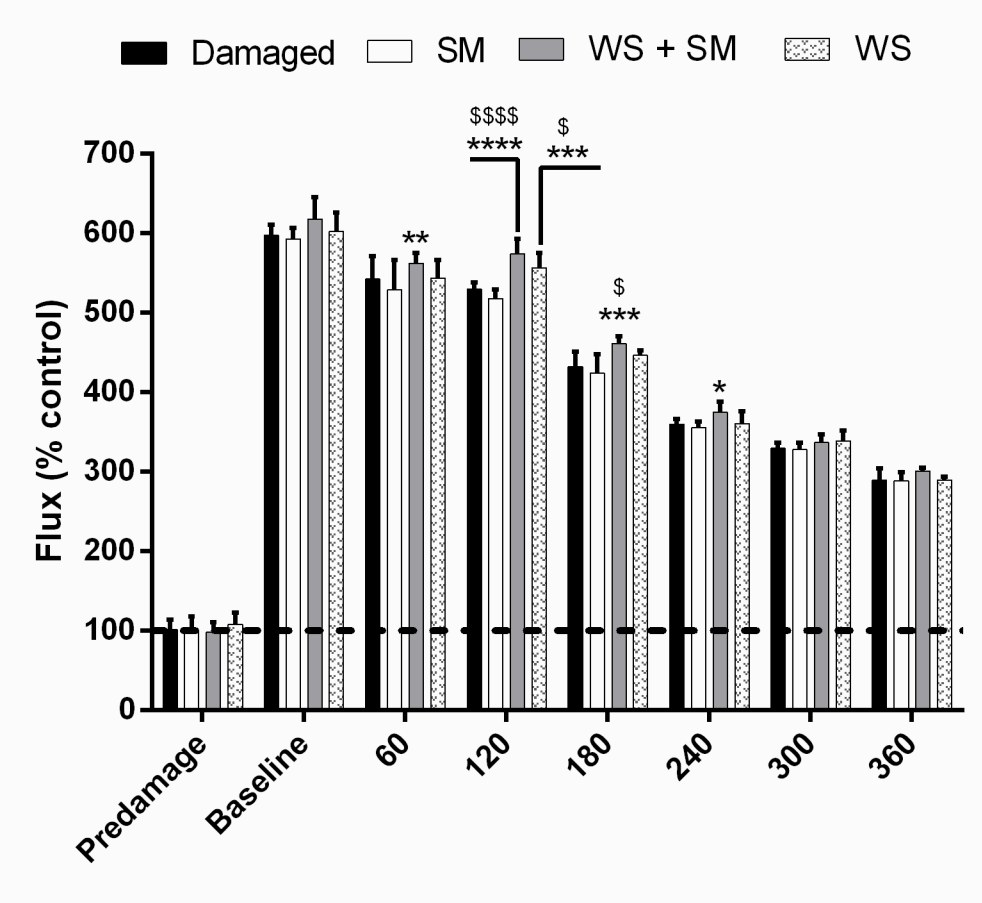
Damaged
SM
WS + SM
WS
Flux (% control)
700
600
500
400
300
200
100
0
$$$$
****
$
***
**
$
***
*
Predamage
Baseline
60
120
180
240
300
360

Figure 4

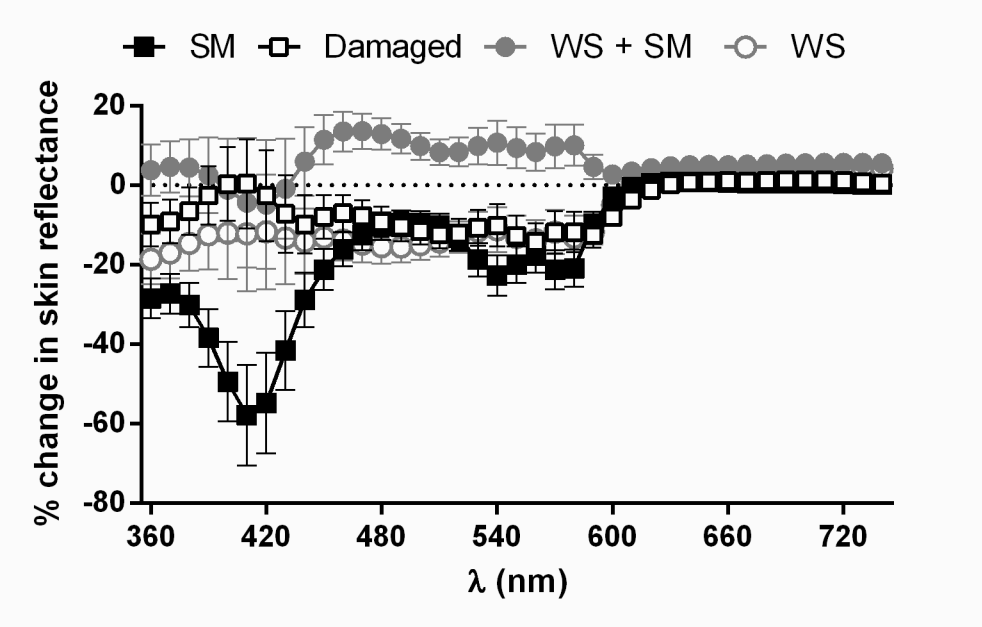
SM
Damaged
WS + SM
WS
% change in skin reflectance
20
0
-20
-40
-60
-80
360
420
480
540
600
660
720
λ (nm)

Figure 5

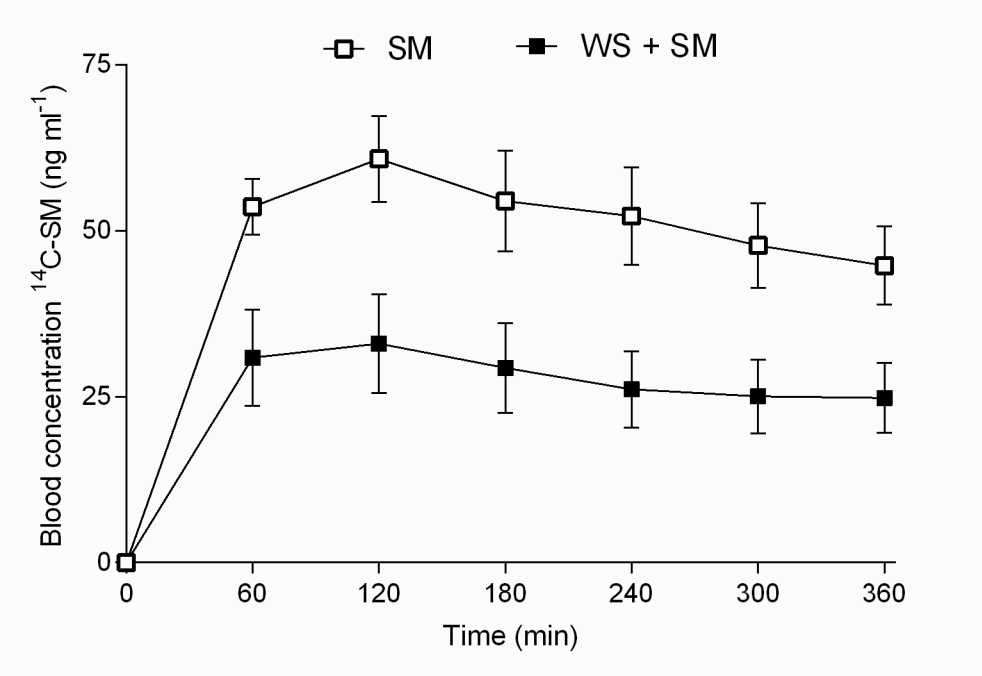
SM
WS + SM
75
50
25
0
Blood concentration ^{14}C-SM (ng ml^{-1})
0
60
120
180
240
300
360
Time (min)

Figure 6

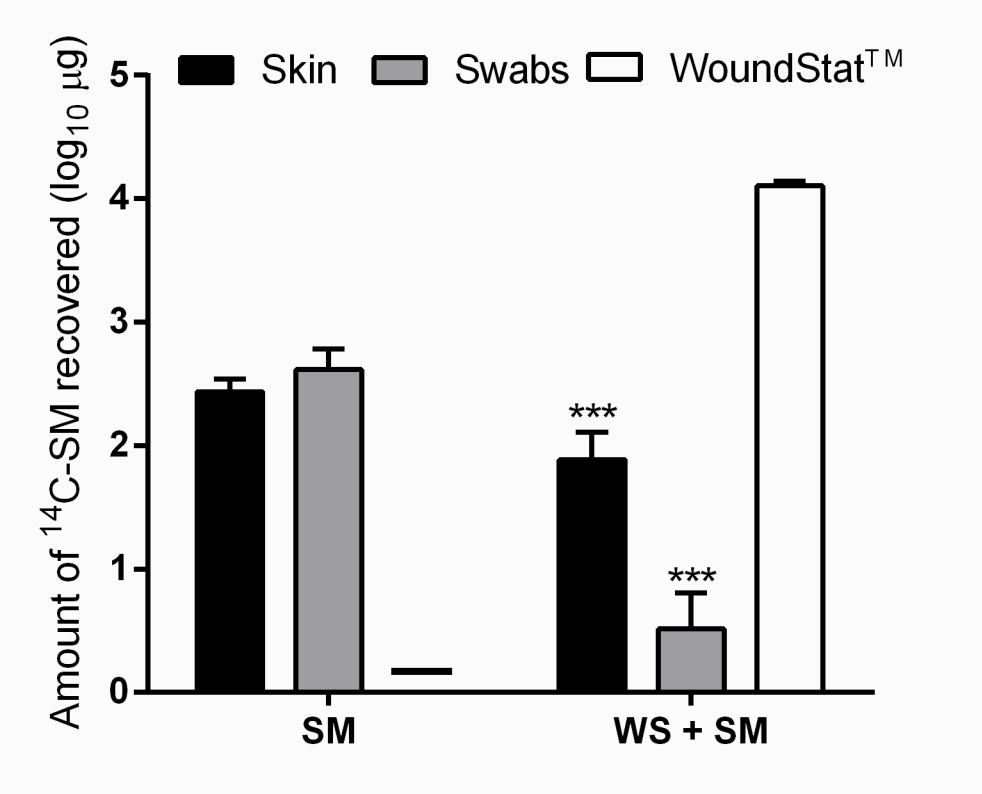
Skin
Swabs
WoundStat™
Amount of ^{14}C-SM recovered (log_{10} µg)
5
4
3
2
1
0
***
***
SM
WS + SM

Figure 7

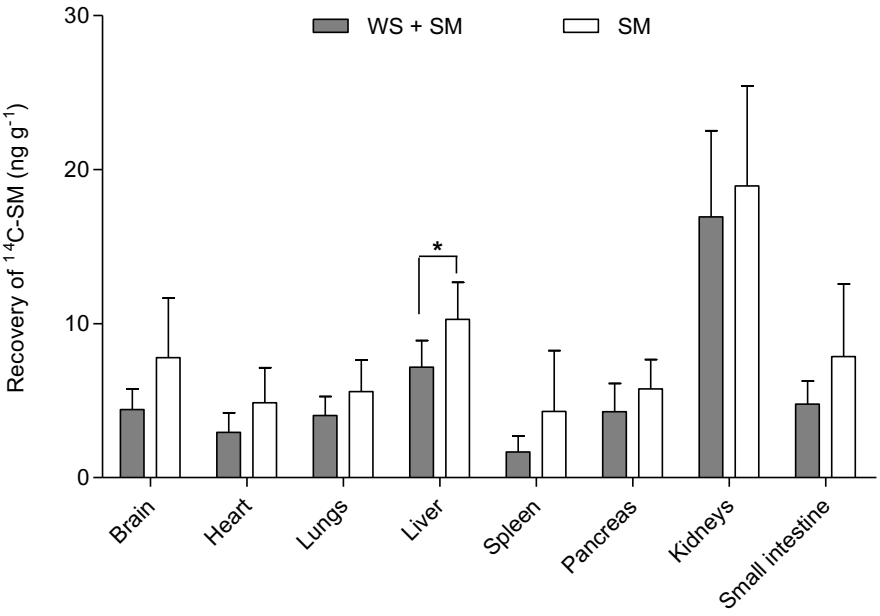
WS + SM
SM
Recovery of ^{14}C-SM (ng g^{-1})
30
20
10
0
*
Brain
Heart
Lungs
Liver
Spleen
Pancreas
Kidneys
Small intestine

Figure 8